Passivity-based Synchronized Visual Feedback Control for Eye-to-Hand Systems

Toshiyuki Murao
Master Program of Innovation for Design and Engineering
Advanced Institute of Industrial Technology
Tokyo 140-0011, Japan
murao-toshiyuki@aiit.ac.jp

Hiroyuki Kawai
Department of Robotics
Kanazawa Institute of Technology
Ishikawa 921-8501, Japan
hiroyuki@neptune.kanazawa-it.ac.jp

Masayuki Fujita
Department of Mechanical and Control Engineering
Tokyo Institute of Technology
Tokyo 152-8550, Japan
fujita@ctrl.titech.ac.jp

***Abstract*—This paper investigates passivity based synchronized visual feedback control for eye-to-hand systems. Firstly the brief summary of the estimation and the control error systems is given with the basic representation of a relative rigid body motion. Secondly we construct the synchronized visual feedback system with an eye-to-hand configuration by combining a synchronization error system. Next, we derive the passivity of the synchronized visual feedback system. Based on passivity and dissipative systems theory, stability and L_2-gain performance analysis are discussed. Finally the validity of the proposed control law can be confirmed by the simulation results.**

I. INTRODUCTION

Robotics and intelligent machines need sensory information to behave autonomously in dynamical environments. Visual information is particularly suited to recognize unknown surroundings. In this sense, vision is one of the highest sensing modalities that currently exist. Vision based control of robotic systems involves the fusion of robot kinematics, dynamics, and computer vision to control the motion of the robot in an efficient manner. The combination of mechanical control with visual information, so-called visual feedback control is important when we consider a mechanical system working in dynamical environments [1][2].

In classical visual servoing, many practical methods are reported by two well known approaches with two camera configurations, i.e., position-based visual feedback control and image-based one with an eye-in-hand configuration or an eye-to-hand (fixed camera) one [1]. Recently, new camera configurations combined each classical one have been proposed. Flandin $et\ al.$ [3] addressed an eye-in-hand and an eye-to-hand cooperation approach that each camera information is partitioned into the positioning task and the orientation one, respectively. In [4], the occlusion problem has been tackled by using multi eye-in-hand and eye-to-hand cameras. The authors discussed passivity based visual feedback control in the 3D (three dimensional) workspace with an eye-in/to-hand configuration which consists of a robot manipulator (a work manipulator) and a camera that is attached to the end-effector of another robot manipulator (a camera manipulator) [5][6]. A common feature among these visual feedback systems with a new camera configuration [3]–[6] is to consist of multiple robot manipulators.

On the other hand, some efforts have recently been made to design multicomposed system which is shared information among robot manipulators. Especially, the mutual synchronized control problem can be formulated as to design interconnections and controllers for the robot manipulators in the system, such that the motion of the manipulator has to be synchronized with respect to not only the desired trajectory but also the motion of other manipulators. In production process tasks that cannot be carried out by a single robot, either because of the complexity of the task or limitations of the robot, the use of multirobot systems working in mutual synchronization, e.g., cooperative schemes, has proved to be a good alternative [7]. One of the advantages of synchronized control is that the controller can reduce the magnitude of the error for the whole system in the transient stage because of synchronous manner, in adding disturbance to some manipulators.

One recent representative work on synchronization of robot manipulators is in [7]. In this work, a scheme which needs only position measurements was proposed to solve the problem of position synchronization of multiple cooperative robot systems, and the controller was shown to be semi-globally exponentially stable. In [8], a leader-follower synchronization output feedback control scheme for the ship replenishment problem was proposed. Chung $et\ al.$ [9] provided a method that eliminates both the all-to-all coupling and the feedback of the acceleration terms. Sun $et\ al.$ designed an adaptive cross-coupled controller [10] and a model-free one [11] to stabilize multi-axis motions for synchronizing mechanical systems. Visual feedback, however, is not considered here. The scheme, which applies to mutual synchronized control for the aforementioned visual feedback system with multiple robot manipulators, should allow us to extend the technological application area.

This paper deals with synchronized visual feedback control for eye-to-hand systems as depicted in Fig. 1. In this paper, for simplicity, the synchronized visual feedback system consists of only two manipulators and a fixed camera, while it can

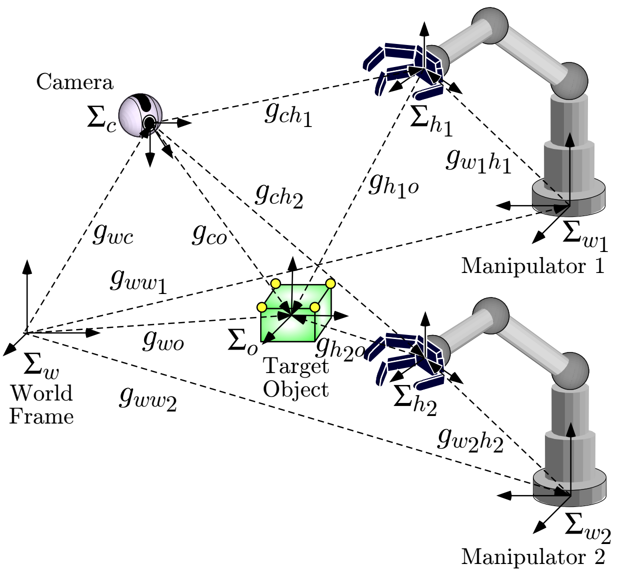

Fig. 1. Synchronized visual feedback system with eye-to-hand configuration.

be easily extended the system which consists of more manipulators and/or a movable camera [5][6]. In our proposed system, not only the convergence of the relative rigid body motion from the hand to the target object to the desired one, but also that of between manipulators are guaranteed, since the synchronization error system is constructed. Based on passivity and dissipative systems theory, stability and L_2-gain performance analysis for the synchronized visual feedback system are discussed. Finally simulation results are shown to verify the stability and the performance of the proposed method.

II. Estimation and Control Error Systems

Throughout this paper, we use the notation $e^{\hat{\xi}\theta_{ab}} \in \mathcal{R}^{3\times 3}$ to represent the change of the principle axes of a frame Σ_b relative to a frame Σ_a. $\xi_{ab} \in \mathcal{R}^3$ specifies the direction of rotation and $\theta_{ab} \in \mathcal{R}$ is the angle of rotation. For simplicity we use $\hat{\xi}\theta_{ab}$ to denote $\hat{\xi}_{ab}\theta_{ab}$. The notation '$\wedge$' (wedge) is the skew-symmetric operator such that $\hat{\xi}\theta = \xi \times \theta$ for the vector cross-product $\times$ and any vector $\theta \in \mathcal{R}^3$. The notation '$\vee$' (vee) denotes the inverse operator to '$\wedge$', i.e., $so(3) \to \mathcal{R}^3$. Recall that a skew-symmetric matrix corresponds to an axis of rotation (via the mapping $a \mapsto \hat{a}$). We use the 4×4 matrix

$$g_{ab} = \begin{bmatrix} e^{\hat{\xi}\theta_{ab}} & p_{ab} \\ 0 & 1 \end{bmatrix} \tag{1}$$

as the homogeneous representation of $g_{ab} = (p_{ab}, e^{\hat{\xi}\theta_{ab}}) \in SE(3)$ describing the configuration of a frame Σ_b relative to a frame Σ_a. The adjoint transformation associated with g_{ab} is denoted by $\mathrm{Ad}_{(g_{ab})}$ [12].

A. Generation of Desired Relative Rigid Body Motion

The visual feedback system considered in this paper has two robot manipulators and a fixed camera as depicted in Fig. 1, where the coordinate frames Σ_w, Σ_c, Σ_o Σ_{w_i} and Σ_{h_i} represent the world frame, the camera frame, the object frame, the base frame of the *i*-th manipulator, and the *i*-th hand (end-effector of the *i*-th manipulator) frame, respectively. Here, the subscript i denotes the index of the manipulators, i.e. $i = 1, 2$ in this paper. Then, the relative rigid body motion from Σ_c to Σ_o can be represented by g_{co}. Similarly, the rigid body motions g_{wc}, g_{wo}, g_{ww_1} and g_{ww_2}, and the relative rigid body motions g_{ch_1}, g_{ch_2}, $g_{w_1h_1}$, $g_{w_2h_2}$, g_{h_1o} and g_{h_2o} are represented, respectively, as shown in Fig. 1.

The objective of synchronized visual feedback control is that both manipulators track the target object while the manipulators should mutually synchronize. In other words, it is to bring the actual relative rigid body motions g_{h_1o} and g_{h_2o} to given constant desired ones g_{h_1d} and g_{h_2d}, respectively. It should be noted that the desired motions g_{h_1d} and g_{h_2d} are related each other because of the mutual synchronous behavior. Therefore, we state how to set the desired rigid body motions for synchronized visual feedback control.

Firstly, we consider the reference manipulator as depicted in Fig. 2, which is the fundamental manipulator to track the target object. The desired value of the synchronized visual feedback system has only one degree of freedom. We define it as g_{hd} which is the relative rigid body motion from the reference hand frame Σ_h to the object frame Σ_o. Next, we set the reference target objects which have the coordinate frames Σ_{o_i} as depicted in Fig. 2, to fulfill $g_{w_io_i} = g_{wo}$ (This means $g_{oo_i} = g_{ww_i}$, too.). Meanwhile, if the control objective is achieved, the motion of all manipulators is corresponded to the reference manipulator i.e. $g_{w_ih_i} = g_{wh}$ because of the mutual synchronous behavior. This means to satisfy the relationship $g_{hh_i} = g_{ww_i}$, too. Hence, we can set $g_{h_id_i}$ using g_{hd} as follows:

$$g_{h_id_i} = g_{ww_i}^{-1} g_{hd} g_{ww_i}. \tag{2}$$

We define the control error g_{eh_i} between the actual relative rigid body motion $g_{h_io_i}$ and the desired one $g_{h_id_i}$ as

$$g_{eh_i} = g_{h_id_i}^{-1} g_{h_io_i}, \tag{3}$$

in other words, $p_{eh_i} = e^{-\hat{\xi}\theta_{h_id_i}}(p_{h_io_i} - p_{h_id_i})$ and $e^{\hat{\xi}\theta_{eh_i}} = e^{-\hat{\xi}\theta_{h_id_i}} e^{\hat{\xi}\theta_{h_io_i}}$. Note that $p_{h_id_i} = p_{h_io_i}$ and $e^{\hat{\xi}\theta_{h_io_i}} = e^{\hat{\xi}\theta_{h_id_i}}$ iff $g_{eh_i} = I_4$, i.e., $p_{eh_i} = 0$ and $e^{\hat{\xi}\theta_{eh_i}} = I_3$. Using the notation $e_R(e^{\hat{\xi}\theta_{ab}}) := \frac{1}{2}(e^{\hat{\xi}\theta_{ab}} - e^{-\hat{\xi}\theta_{ab}})^\vee$ which denotes the error vector of the rotation matrix $e^{\hat{\xi}\theta_{ab}}$, the vector of the control error is given by

$$e_{h_i} := \begin{bmatrix} p_{eh_i}^T & e_R^T(e^{\hat{\xi}\theta_{eh_i}}) \end{bmatrix}^T. \tag{4}$$

Note that $e_{h_i} = 0$ iff $p_{eh_i} = 0$ and $e^{\hat{\xi}\theta_{eh_i}} = I_3$. Therefore, if the vector of the control error is equal to zero, then the actual relative rigid body motion $g_{h_io_i}$ equals the desired relative rigid body motion $g_{h_id_i}$.

B. Basic Representation for Visual Feedback System and Estimation Error System

This subsection mainly reviews our previous works [13][14] via the passivity based visual feedback control.

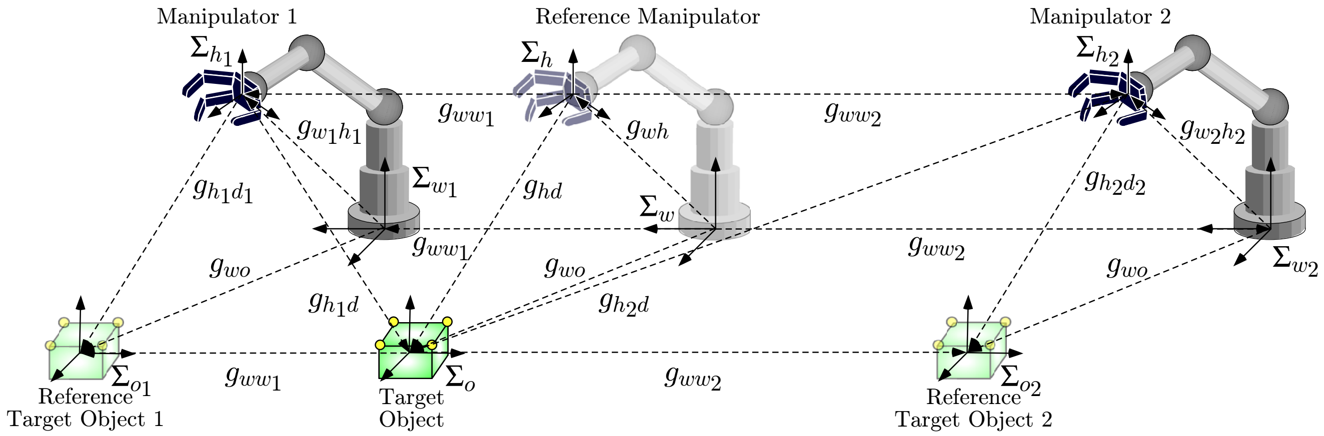

Fig. 2. Generation of desired relative rigid body motion.

In order to achieve the control objective, the relative rigid body motion $g_{h_io_i}$ is needed. $g_{h_io_i}$ can be represented as follows:

$$g_{h_io_i} = g_{ch_i}^{-1} g_{co} g_{ww_i}. \tag{5}$$

In (5), since g_{ch_i} and g_{ww_i} can be given by the measured information, we consider to get the relative rigid body motion g_{co}[1]. The relative rigid body motion from Σ_c to Σ_o can be led by using the composition rule for rigid body transformations ([12], Chap. 2, pp. 37, eq. (2.24)) as follows:

$$g_{co} = g_{wc}^{-1} g_{wo}. \tag{6}$$

The relative rigid body motion involves the velocity of each rigid body. To this aid, let us consider the velocity of a rigid body as described in [12]. We define the body velocity of the camera relative to the world frame Σ_w as $V_{wc}^b = [v_{wc}^T \ \omega_{wc}^T]^T$, where v_{wc} and ω_{wc} represent the velocity of the origin and the angular velocity from Σ_w to Σ_c, respectively ([12] Chap. 2, eq. (2.55)).

Differentiating (6) with respect to time, the body velocity of the relative rigid body motion g_{co} can be written as follows (See [13]):

$$V_{co}^b = -\mathrm{Ad}_{(g_{co}^{-1})} V_{wc}^b + V_{wo}^b \tag{7}$$

where V_{wo}^b is the body velocity of the target object relative to Σ_w. Eq. (7) is the basic representation for the three coordinate frames of the visual feedback system [13]. In the case of the fixed camera configuration, i.e. $V_{wc}^b = 0$, the body velocity of the relative rigid body motion g_{co} can be rewritten as

$$V_{co}^b = V_{wo}^b. \tag{8}$$

Roughly speaking, if both the camera and the target object move, then the relative rigid body motion g_{co} will be derived from the difference between the camera velocity V_{wc}^b and the target object velocity V_{wo}^b. Hence, the model of the relative rigid body motion from Σ_c to Σ_o equals the target object velocity V_{wo}^b.

[1]We assume that g_{wc} and g_{wh_i} can be obtained accurately by a prior calibration procedure.

The visual feedback control task requires information of the relative rigid body motion g_{co}. Since the measurable information is only the image information $f(g_{co})$ in the visual feedback system, we consider a nonlinear observer in order to estimate the relative rigid body motion g_{co} from the image information $f(g_{co})$.

Firstly, using (8), we choose estimates $\bar{g}_{co}$ and $\bar{V}_{co}^b$ of the relative rigid body motion and velocity, respectively as

$$\bar{V}_{co}^b = u_e. \tag{9}$$

The new input u_e is to be determined in order to drive the estimated values $\bar{g}_{co}$ and $\bar{V}_{co}^b$ to their actual values.

In order to establish the estimation error system, we define the estimation error between the estimated value $\bar{g}_{co}$ and the actual relative rigid body motion g_{co} as

$$g_{ee} = \bar{g}_{co}^{-1} g_{co}. \tag{10}$$

Using the notation $e_R(e^{\hat{\xi}\theta_{ab}})$, the vector of the estimation error is defined as

$$e_e := \left[\begin{array}{cc} p_{ee}^T & e_R^T(e^{\hat{\xi}\theta_{ee}}) \end{array} \right]^T. \tag{11}$$

Therefore, if the vector of the estimation error is equal to zero, then the estimated relative rigid body motion $\bar{g}_{co}$ equals the actual relative rigid body motion g_{co}.

Suppose the attitude estimation error θ_{ee} is small enough that we can let $e^{\hat{\xi}\theta_{ee}} \simeq I + \mathrm{sk}(e^{\hat{\xi}\theta_{ee}})$. Therefore, using a first-order Taylor expansion approximation, the estimation error vector e_e can be obtained from image information $f(g_{co})$ and the estimated value of the relative rigid body motion $\bar{g}_{co}$ as follows ([13]):

$$e_e = J^{\dagger}(\bar{g}_{co})(f - \bar{f}), \tag{12}$$

where $\bar{f}$ is the estimated value of image information. In the same way as the basic representation (7), the estimation error system can be represented by

$$V_{ee}^b = -\mathrm{Ad}_{(g_{ee}^{-1})} u_e + V_{wo}^b. \tag{13}$$

It should be noted that if the vector of the estimation error is equal to zero, then the estimated relative rigid body motion $\bar{g}_{co}$ equals the actual one g_{co}.

C. Control Error System

In this subsection which mainly reviews our previous work [6], let us consider the dual of the estimation error system, which we call the control error system.

In order to achieve the control objective, we have to derive g_{eh_i} defined as (3). Using g_{ee}, the control error can be transformed as

$$\begin{aligned} g_{eh_i} &= g_{h_id_i}^{-1} g_{h_io_i} = g_{h_id_i}^{-1} g_{ch_i}^{-1} g_{co} g_{ww_i} \\ &= g_{h_id_i}^{-1} g_{ch_i}^{-1} \bar{g}_{co} g_{ee} g_{ww_i}. \end{aligned} \tag{14}$$

In (14), $g_{h_id_i}$, g_{ch_i}, $\bar{g}_{co}$ and g_{ww_i} are known information. While the estimation error vector e_e can be obtained as (12), the estimation error matrix g_{ee} cannot be directly obtained, because g_{ee} is defined using non-measurable value g_{co} as (10). Therefore, we derive g_{ee} from e_e.

Because of the definition of the estimation error vector e_e, i.e., $e_e := [p_{ee}^T \ e_R^T(e^{\hat{\xi}\theta_{ee}})]^T$, the position estimation error p_{ee} can be derived directly from e_e. Under the condition $-\frac{\pi}{2} \leq \theta_{ee} \leq \frac{\pi}{2}$, $\xi\theta_{ee}$ can be derived as follows [6]:

$$\xi\theta_{ee} = \frac{\sin^{-1} \|e_R(e^{\hat{\xi}\theta_{ee}})\|}{\|e_R(e^{\hat{\xi}\theta_{ee}})\|} e_R(e^{\hat{\xi}\theta_{ee}}). \tag{15}$$

Hence, g_{ee} can be derived from e_e through $\xi\theta_{ee}$.

The reference of the relative rigid body motion $g_{h_id_i}$ is constant in this paper, i.e., $\dot{g}_{h_id_i} = 0$, hence, $V_{eh_i}^b = V_{h_io_i}^b$. Thus, differentiating (3) with respect to time, the control error system can be represented as

$$V_{eh_i}^b = -\mathrm{Ad}_{(g_{eh_i}^{-1})} \mathrm{Ad}_{(g_{h_id_i}^{-1})} V_{wh_i}^b + V_{wo}^b. \tag{16}$$

This is dual to the estimation error system.

III. Passivity-based Synchronized Visual Feedback Control

For assembly tasks in modern manufacturing and space applications, a scheme which reduces not only the error concerning the control objective but also that of synchronous manner must have the great potential [10]. For the visual feedback system which consists of two manipulators and a fixed camera shown as Fig. 1, the straightforward extension of the controller using only the estimation and the control error systems in [14] can be also proposed without synchronous manner. However, although it can be treated the tracking problem, it can not be ensured the synchronous behavior. This section considers synchronized visual feedback control based on passivity which is a main contribution in this paper.

A. Synchronization Error System

In this subsection, we derive the synchronization error system in order to impose the synchronous manner. Firstly, we define the error $g_{eh_{ij}} = (p_{eh_{ij}}, e^{\hat{\xi}\theta_{eh_{ij}}})$ between the relative rigid body motion of the one manipulator $g_{h_io_i}$ and that of another manipulator $g_{h_jo_j}$ as

$$g_{eh_{ij}} = g_{h_jo_j}^{-1} g_{h_io_i}, \ (i,j) = (1,2),(2,1). \tag{17}$$

Moreover, the synchronization error is defined using the element of the predefined error (17) and the coupling gains which denote the interactions between the manipulators in the system as follows:

$$g_{es_{ij}} = \begin{bmatrix} k_{R_{ij}} e^{\hat{\xi}\theta_{eh_{ij}}} & k_{p_{ij}} p_{eh_{ij}} \\ 0 & 1 \end{bmatrix} \tag{18}$$

where $k_{p_{ij}}$ is the coupling gain for the position and $k_{R_{ij}}$ is that for the rotation. Using the notation $e_R(e^{\hat{\xi}\theta_{ab}})$, the synchronization error vector is defined as

$$e_{s_{ij}} := \begin{bmatrix} p_{es_{ij}}^T & e_R^T(e^{\hat{\xi}\theta_{es_{ij}}}) \end{bmatrix}^T. \tag{19}$$

Differentiating (18) with respect to time, the synchronization error system can be represented as

$$\begin{aligned} V_{es_{ij}}^b =& -K_{s_{ij}} \mathrm{Ad}_{(g_{eh_i}^{-1})} \mathrm{Ad}_{(g_{h_id_i}^{-1})} V_{wh_i}^b \\ &+ K_{s_{ij}} \mathrm{Ad}_{(g_{h_io_i}^{-1} \cdot g_{h_jd_j})} \mathrm{Ad}_{(g_{h_jd_j}^{-1})} V_{wh_j}^b \\ &+ K_{s_{ij}} \mathrm{Ad}_{(g_{ww_i}^{-1})} \left(I - \mathrm{Ad}_{(g_{h_io}^{-1} \cdot g_{h_jo})} \right) V_{wo}^b, \end{aligned} \tag{20}$$

where $K_{s_{ij}} := \mathrm{diag}\{k_{p_{ij}} k_{R_{ij}} I, k_{R_{ij}}^2 I\}$ for all $i, j = 1, 2, i \neq j$.

B. Synchronized Visual Feedback System

The dynamics of the rigid body manipulators can be written as

$$M_i(q_i)\ddot{q}_i + C_i(q_i,\dot{q}_i)\dot{q}_i + g_i(q_i) = \tau_i + \tau_{id} \tag{21}$$

where $M_i \in \mathcal{R}^{n\times n}$ is the inertia matrix, $C_i \in \mathcal{R}^{n\times n}$ is the Coriolis matrix, $g_i \in \mathcal{R}^n$ is the gravity vector, and q_i, $\dot{q}_i$ and $\ddot{q}_i$ are the joint angle, velocity and acceleration, respectively. τ_i is the vector of the input torque, and τ_{id} represents a disturbance input. Since the manipulator dynamics is considered, the hand body velocity is given by $V_{wh_i}^b = J_{ib}(q_i)\dot{q}_i$, where $J_{ib}(q_i)$ is the body manipulator Jacobian [12].

Next, we propose the control law for the manipulator as

$$\begin{aligned} \tau_i =& M_i(q_i)\ddot{q}_{id} + C_i(q_i,\dot{q}_i)\dot{q}_{id} + g_i(q_i) \\ &+ J_{ib}^T(q_i)\mathrm{Ad}_{(g_{h_id_i}^{-1})}^T e_{h_i} + J_{ib}^T(q_i)\mathrm{Ad}_{(g_{h_jo_j}^{-1})}^T K_{s_{ij}} e_{s_{ij}} \\ &- J_{ib}^T(q_i)\mathrm{Ad}_{(g_{h_io_i}^{-1})}^T K_{s_{ji}} e_{s_{ji}} + u_{\xi_i} \end{aligned} \tag{22}$$

where $\dot{q}_{id}$ and $\ddot{q}_{id}$ represent the desired joint velocity and acceleration, respectively. The new input u_{ξ_i} is to be determined in order to achieve the control objective.

Let us define the error vector with respect to the joint velocity of the manipulator as

$$\xi_i := \dot{q}_i - \dot{q}_{id}. \tag{23}$$

Moreover, we design the reference of the joint velocity as $\dot{q}_{id} := J_{ib}^\dagger(q_i) u_{h_id}$ where u_{h_id} is the desired body velocity which will be obtained from the aforementioned error systems. Thus, $V_{wh_i}^b$ should be replaced by u_{h_id}.

Using (13), (16) and (20)–(22), the synchronized visual feedback system can be derived as the equation (24) at the bottom of the next page, where the input $u := [u_{\xi_1}^T \ u_{\xi_2}^T \ (\mathrm{Ad}_{(g_{h_1d_1}^{-1})} u_{h_1d})^T \ (\mathrm{Ad}_{(g_{h_2d_2}^{-1})} u_{h_2d})^T \ u_e^T]^T$. We define the state and the disturbance of the synchronized visual feedback system as $x := [\xi_1^T\ \xi_2^T\ e_{h_1}^T\ e_{h_2}^T\ e_{s_{12}}^T\ e_{s_{21}}^T\ e_e^T]^T$ and $w := [\tau_{1d}^T\ \tau_{2d}^T\ (V_{wo}^b)^T]^T$, respectively.

Remark 1: If the coupling gains $k_{p_{ij}} = k_{R_{ij}} = 0$ and the synchronization error $e_{s_{ij}}$ is not considered, then the synchronized visual feedback system (24) can be regarded as the non-synchronized one which consists of two manipulators and a fixed camera. Non-synchronized system is a straightforward extension of the eye-to-hand visual feedback system [14]. Thus, the visual feedback system with the eye-to-hand configuration [14] is included as the special case of the system (24).

C. Passivity of Synchronized Visual Feedback System

Before proposing a synchronized visual feedback control law, we derive an important lemma.

Lemma 1: If $w = 0$, then the synchronized visual feedback system (24) satisfies

$$\int_0^T u^T \nu \geq -\beta, \quad {}^\forall T > 0 \tag{25}$$

where

$$\begin{aligned}
\nu &:= NK_s x \\
N &= \begin{bmatrix} I & 0 & 0 & 0 & 0 & 0 & 0 \\ 0 & I & 0 & 0 & 0 & 0 & 0 \\ 0 & 0 & -I & 0 & -\mathrm{Ad}^T_{(g^{-1}_{h_2o_2}\cdot g_{h_1d_1})} & \mathrm{Ad}^T_{(g^{-1}_{eh_1})} & 0 \\ 0 & 0 & 0 & -I & \mathrm{Ad}^T_{(g^{-1}_{eh_2})} & -\mathrm{Ad}^T_{(g^{-1}_{h_1o_1}\cdot g_{h_2d_2})} & 0 \\ 0 & 0 & 0 & 0 & 0 & 0 & -I \end{bmatrix} \\
K_s &= \mathrm{diag}\{I, I, I, I, K_{s_{12}}, K_{s_{21}}, I\}
\end{aligned}$$

and β is a positive scalar.

Proof: Consider the following positive definite function

$$\begin{aligned}
V = \frac{1}{2}\xi_1^T M_1 \xi_1 + \frac{1}{2}\xi_2^T M_2 \xi_2 + E(g_{eh_1}) + E(g_{eh_2}) \\
+ \frac{1}{k_{R_{12}}} E(g_{es_{12}}) + \frac{1}{k_{R_{21}}} E(g_{es_{21}}) + E(g_{ee}),
\end{aligned} \tag{26}$$

where $E(g_{ab}) := \frac{1}{2}\|p_{ab}\|^2 + \phi(e^{\hat{\xi}\theta_{ab}})$ and $\phi(e^{\hat{\xi}\theta_{ab}}) := \frac{1}{2}\mathrm{tr}(I - e^{\hat{\xi}\theta_{ab}})$ is the error function of the rotation matrix (see, e.g., [15]). Differentiating (26) with respect to time yields

$$\begin{aligned}
\dot{V} &= \frac{1}{2}\xi_1^T \dot{M}_1 \xi_1 + \frac{1}{2}\xi_2^T \dot{M}_2 \xi_2 \\
&\quad + x^T \begin{bmatrix} M_1 & 0 & 0 & 0 & 0 & 0 & 0 \\ 0 & M_2 & 0 & 0 & 0 & 0 & 0 \\ 0 & 0 & \mathrm{Ad}_{(e^{\hat{\xi}\theta_{eh_1}})} & 0 & 0 & 0 & 0 \\ 0 & 0 & 0 & \mathrm{Ad}_{(e^{\hat{\xi}\theta_{eh_2}})} & 0 & 0 & 0 \\ 0 & 0 & 0 & 0 & \mathrm{Ad}_{(e^{\hat{\xi}\theta_{eh_{12}}})} & 0 & 0 \\ 0 & 0 & 0 & 0 & 0 & \mathrm{Ad}_{(e^{\hat{\xi}\theta_{eh_{21}}})} & 0 \\ 0 & 0 & 0 & 0 & 0 & 0 & \mathrm{Ad}_{(e^{\hat{\xi}\theta_{ee}})} \end{bmatrix} \begin{bmatrix} \dot{\xi}_1 \\ \dot{\xi}_2 \\ V^b_{eh_1} \\ V^b_{eh_2} \\ V^b_{es_{12}} \\ V^b_{es_{21}} \\ V^b_{ee} \end{bmatrix} \\
&= x^T K_s N^T u,
\end{aligned} \tag{27}$$

using the skew-symmetry of the matrices $\hat{p}_{eh_1}$, $\hat{p}_{eh_2}$, $\hat{p}_{eh_{12}}$, $\hat{p}_{eh_{21}}$, $\hat{p}_{ee}$, $\dot{M}_1 - 2C_1$ and $\dot{M}_2 - 2C_2$. Note that we have utilized the fact that $e_R(k_{R_{ij}} e^{\hat{\xi}\theta_{ab}}) = k_{R_{ij}} e_R(e^{\hat{\xi}\theta_{ab}})$. Integrating (27) from 0 to T, we obtain

$$\int_0^T u^T \nu d\tau = V(T) - V(0) \geq -V(0) = -\beta \tag{28}$$

where β is a positive scalar that only depends on the initial states of ξ_1, ξ_2, e_{h_1}, e_{h_2}, $e_{s_{12}}$, $e_{s_{21}}$ and e_e. ■

Remark 2: Lemma 1 would suggest that the synchronized visual feedback system is passive from the input u to the output ν as in the definition in [16]. Note that Lemma 1 can be shown to connect with the each passivity property of the manipulator dynamics, the estimation error system, the control error system and the synchronization error system.

D. Stability Analysis for Synchronized Visual Feedback System

We now propose the following control input for the interconnected system:

$$\begin{aligned}
u &= -K\nu = -KNK_s x \\
K &:= \mathrm{diag}\{K_{\xi_1}, K_{\xi_2}, K_{h_1}, K_{h_2}, K_e\}
\end{aligned} \tag{29}$$

$$\begin{aligned}
\begin{bmatrix} \dot{\xi}_1 \\ \dot{\xi}_2 \\ V^b_{eh_1} \\ V^b_{eh_2} \\ V^b_{es_{12}} \\ V^b_{es_{21}} \\ V^b_{ee} \end{bmatrix} &= \begin{bmatrix} -M_1^{-1}C_1\xi_1 + M_1^{-1}J_{1b}^T\left(\mathrm{Ad}^T_{(g^{-1}_{h_1d_1})} e_{h_1} + \mathrm{Ad}^T_{(g^{-1}_{h_2o_2})} K_{s_{12}} e_{s_{12}} - \mathrm{Ad}^T_{(g^{-1}_{h_1o_1})} K_{s_{21}} e_{s_{21}}\right) \\ -M_2^{-1}C_2\xi_2 + M_2^{-1}J_{2b}^T\left(\mathrm{Ad}^T_{(g^{-1}_{h_2d_2})} e_{h_2} + \mathrm{Ad}^T_{(g^{-1}_{h_1o_1})} K_{s_{21}} e_{s_{21}} - \mathrm{Ad}^T_{(g^{-1}_{h_2o_2})} K_{s_{12}} e_{s_{12}}\right) \\ -\mathrm{Ad}_{(g^{-1}_{h_1o_1})} J_{1b}\xi_1 \\ -\mathrm{Ad}_{(g^{-1}_{h_2o_2})} J_{2b}\xi_2 \\ -K_{12}\mathrm{Ad}_{(g^{-1}_{h_1o_1})}(J_{1b}\xi_1 - J_{2b}\xi_2) \\ -K_{21}\mathrm{Ad}_{(g^{-1}_{h_2o_2})}(J_{2b}\xi_2 - J_{1b}\xi_1) \\ 0 \end{bmatrix} \\
&\quad + \begin{bmatrix} M_1^{-1} & 0 & 0 & 0 & 0 \\ 0 & M_2^{-1} & 0 & 0 & 0 \\ 0 & 0 & -\mathrm{Ad}_{(g^{-1}_{eh_1})} & 0 & 0 \\ 0 & 0 & 0 & -\mathrm{Ad}_{(g^{-1}_{eh_2})} & 0 \\ 0 & 0 & -K_{s_{12}}\mathrm{Ad}_{(g^{-1}_{eh_1})} & K_{s_{12}}\mathrm{Ad}_{(g^{-1}_{h_1o_1}\cdot g_{h_2d_2})} & 0 \\ 0 & 0 & K_{s_{21}}\mathrm{Ad}_{(g^{-1}_{h_2o_2}\cdot g_{h_1d_1})} & -K_{s_{21}}\mathrm{Ad}_{(g^{-1}_{eh_2})} & 0 \\ 0 & 0 & 0 & 0 & -\mathrm{Ad}_{(g^{-1}_{ee})} \end{bmatrix} u + \begin{bmatrix} M_1^{-1} & 0 & 0 \\ 0 & M_2^{-1} & 0 \\ 0 & 0 & I \\ 0 & 0 & I \\ 0 & 0 & K_{s_{12}}\mathrm{Ad}_{(g^{-1}_{ww_1})}\left(I - \mathrm{Ad}_{(g^{-1}_{h_1o}\cdot g_{h_2o})}\right) \\ 0 & 0 & K_{s_{21}}\mathrm{Ad}_{(g^{-1}_{ww_2})}\left(I - \mathrm{Ad}_{(g^{-1}_{h_2o}\cdot g_{h_1o})}\right) \\ 0 & 0 & I \end{bmatrix} w
\end{aligned} \tag{24}$$

where $K_{\xi_i} := \mathrm{diag}\{k_{\xi_i 1}, \cdots, k_{\xi_i n}\}$, $K_{h_i} := \mathrm{diag}\{k_{h_i 1}, \cdots, k_{h_i 6}\}$ and $K_e := \mathrm{diag}\{k_{e1}, \cdots, k_{e6}\}$ denote the positive gain matrices.

Theorem 1: If $w = 0$, then the equilibrium point $x = 0$ for the closed-loop system (24) and (29) is asymptotic stable.

Proof: In the proof of Lemma 1, we have already derived that the time derivative of V along the trajectory of the system (24) is formulated as (27). Using the control input (29), (27) can be transformed into

$$\dot{V} = -x^T K_s N^T K N K_s x. \tag{30}$$

This completes the proof. ■

Theorem 1 guarantees the stability of synchronized control using a Lyapunov function for the eye-to-hand synchronized visual feedback system (24) which is a highly nonlinear system. It is interesting to note that stability analysis is based on passivity as described in (25). For the tasks which need the synchronous manner, the control performance should be improved compared to the eye-to-hand non-synchronized visual feedback control law, because the synchronized control design considers the mutual synchronization error. For the visual feedback system, it is difficult that the desired trajectory in joint space is given explicitly, since the motion of the target object is unknown. Although the synchronization error is defined in the joint space in the previous works [7]–[11], we define it in the work space by making the reference manipulator and the reference target objects as shown in Fig 2.

E. L_2-gain Performance Analysis for Synchronized Visual Feedback System

Based on the dissipative systems theory, we consider L_2-gain performance analysis for the synchronized visual feedback system (24) in one of the typical problems, i.e. the disturbance attenuation problem. Now, let us define

$$P := K_s N^T K N K_s - \frac{1}{2\gamma^2}\|W\|^2 - \frac{1}{2}I \tag{31}$$

where $\gamma \in \mathcal{R}$ is positive and W is defined at the bottom of the next page. Then we have the following theorem.

Theorem 2: Given a positive scalar γ and consider the control input (29) with the gains K_{ξ_1}, K_{ξ_2}, K_{h_1}, K_{h_2} and K_e such that the matrix P is positive semi-definite, then the closed-loop system (24) and (29) has L_2-gain $\leq \gamma$.

The proof is omitted due to space limitations, Theorem 2 can be proved using the energy function (26) as a storage function for L_2-gain performance analysis. The L_2-gain performance analysis of the synchronized visual feedback system is discussed via the dissipative systems theory. In H_∞-type control, we can consider some problems by establishing the adequate generalized plant. This paper has discussed L_2-gain performance analysis for the disturbance attenuation problem. The proposed strategy can be extended for the other-type of generalized plants of the synchronized visual feedback systems.

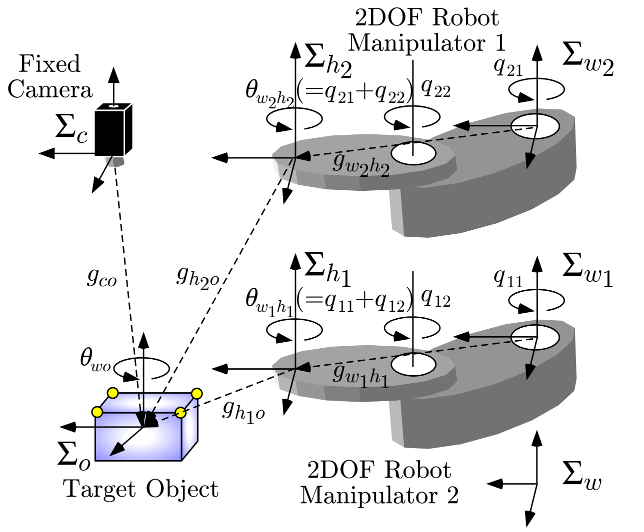

Fig. 3. Coordinated frames for synchronized visual feedback system with two 2DOF manipulators.

IV. Simulations

In this section, the validity of the proposed control law can be confirmed by comparing the simulation results with a static target object. Although we only discuss simulation results, it should be noted that the model parameters were developed using actual synchronized visual feedback system.

The simulation results on two 2DOF manipulators as depicted in Fig. 3 are shown in order to understand our proposed method simply, though it is valid for 3D synchronized visual feedback systems. We defined the seven coordinates which were described in Fig. 3. The target object has four feature points. The control objective is to bring the actual relative rigid body motions g_{h_1o} and g_{h_2o} to a given references g_{h_1d} and g_{h_2d} with the mutual synchronization of robotic manipulation. In other words, it can be stated as the desire to regulate not only the both hand control errors e_{h_1} and e_{h_2} but also the synchronization errors $e_{s_{12}}$ and $e_{s_{21}}$ to zero.

In this paper, we present simulation results for the synchronized visual feedback control, compared with the non-synchronized one which is the straightforward extension of the controller in [14]. The simulation is carried out with the initial condition $q_{11}(0) = \pi/4$ [rad], $q_{12}(0) = \pi/12$ [rad], $q_{21}(0) = \pi/6$ [rad], $q_{22}(0) = -\pi/6$ [rad], $p_{ww_1} = [0\ 0\ -1]^T$ [m], $\xi\theta_{ww_1} = [0\ 0\ 0]^T$ [rad], $p_{ww_2} = [0\ 0\ -2]^T$ [m], $\xi\theta_{ww_2} = [0\ 0\ 0]^T$ [rad], $p_{wc} = [0.4732\ 0.1\ 0]^T$ [m], $\xi\theta_{wc} = [0\ 0\ 0]^T$ [rad], $p_{wo} = [0.3986\ 0\ -3]^T$ [m], $\xi\theta_{wo} = [0\ 0\ -0.5087]^T$ [rad]. The desired relative rigid body motion is $p_{h_1d} = [0\ 0\ -2]^T$ [m], $\xi\theta_{h_1d} = [0\ 0\ 0]^T$ [rad], $p_{h_2d} = [0\ 0\ -1]^T$ [m], $\xi\theta_{h_2d} = [0\ 0\ 0]^T$ [rad], and the initial errors are calculated as $\xi_1(0) = \xi_2(0) = [0\ 0]^T$ [rad/s], $p_{eh_1}(0) = [-0.294\ -0.293\ 0]^T$ [m], $\xi\theta_{eh_1}(0) = [0\ 0\ -1]^T$ [rad], $p_{eh_2}(0) = [-0.075\ -0.1\ 0]^T$ [m], $\xi\theta_{eh_2}(0) = [0\ 0\ -0.487]^T$ [rad], $p_{es12}(0) = [-0.063\ -0.179\ 0]^T$ [m], $\xi\theta_{es12}(0) = [0\ 0\ -0.563]^T$ [rad], $p_{es21}(0) = [-0.124\ -0.144\ 0]^T$ [m],

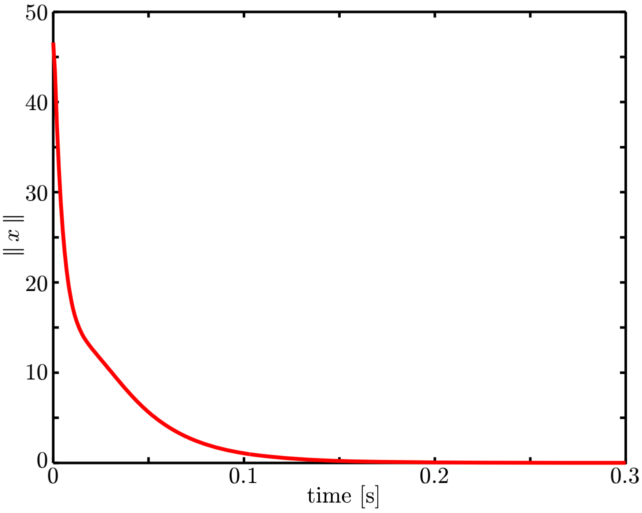

Fig. 4. Norm of the state x with the proposed control law

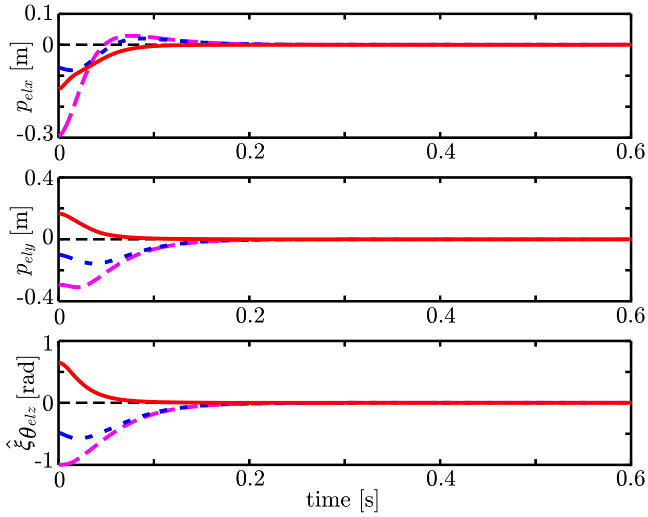

Fig. 5. Control error e_{h_1} (Dashed) and e_{h_2} (Dotted), and the synchronization error $e_{s_{21}}$ (Solid) with the proposed control law

$\xi\theta_{es21}(0) = [0\ 0\ 0.563]^T$ [rad], $p_{ee}(0) = [0\ -0.004\ 0]^T$ [m], $\xi\theta_{ee}(0) = [0\ 0\ -0.015]^T$ [rad], respectively.

The controller parameters for the control law u (29) were empirically selected as $K_{\xi_1} = \mathrm{diag}\{10, 3\}$, $K_{\xi_2} = \mathrm{diag}\{10, 3\}$, $K_{h_1} = \mathrm{diag}\{30, 30, 15, 15, 15, 30\}$, $K_{h_2} = \mathrm{diag}\{30, 30, 15, 15, 15, 30\}$, $K_e = 30I$. The coupling gains for mutual synchronization were chosen as $k_{p_{12}} = k_{R_{12}} = k_{p_{21}} = k_{R_{21}} = 0.75$. When we set the coupling gains, it is important not to select too large values. In the case of the non-synchronized control law, the same gains are set in order to compare the both control laws simply, except for the coupling gains $k_{p_{12}} = k_{R_{12}} = k_{p_{21}} = k_{R_{21}} = 0$.

The simulation results are presented in Figs. 4–6. The norm of the state x applying the proposed control law is shown in Fig. 4. Figs. 5 and 6 illustrate the hand control errors e_{h_1} (Dashed) and e_{h_2} (Dotted), and the synchronization error $e_{s_{21}}$ (Solid), respectively. In these figures, we focus on the errors of the translations of x and y and the rotation of z, because the errors of the translation of z and the rotations of x and y are zeros ideally on the defined coordinates in Fig. 3. Figs. 5 and 6 denote the errors applying the proposed synchronized control law and the non-synchronized one, respectively.

In Figs. 4 and 5, the asymptotic stability applying the proposed control law can be confirmed by steady state performance. Moreover, it can be verified that $e_{s_{21}}$ converges faster than errors of e_{h_1} and e_{h_2} in the synchronized visual feedback

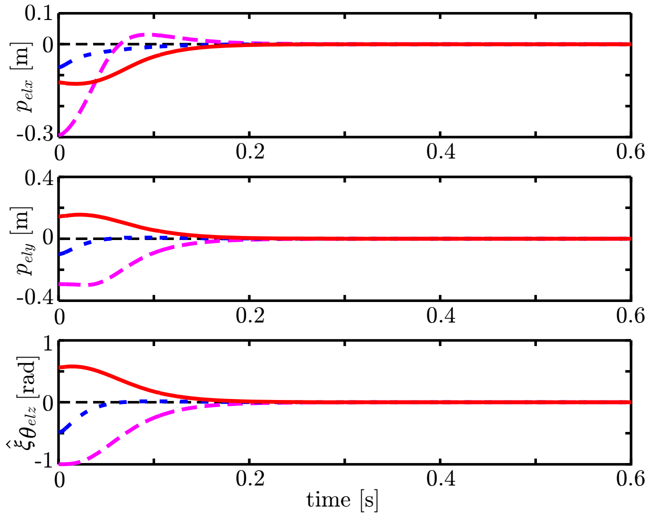

Fig. 6. Control error e_{h_1} (Dashed) and e_{h_2} (Dotted), and the synchronization error $e_{s_{21}}$ (Solid) with the non-synchronized control law

control case in Fig. 5. This proves the mutual synchronization behavior. Meanwhile, the errors e_{h_1} and e_{h_2} converge faster than $e_{s_{21}}$ for the non-synchronized control case in Fig. 6.

Moreover, we tested the system by adding a force disturbance $\tau_{1d} = [100\ 50]^T$ [Nm] to only the manipulator 1 from

$$W := \begin{bmatrix} I & 0 & 0 & 0 & 0 & 0 & 0 \\ 0 & I & 0 & 0 & 0 & 0 & 0 \\ 0 & 0 & \mathrm{Ad}_{(e^{-\hat{\xi}\theta_{eh_1}})} & \mathrm{Ad}_{(e^{-\hat{\xi}\theta_{eh_2}})} & \left(I - \mathrm{Ad}^T_{(g_{h_1o}^{-1}\cdot g_{h_2o})}\right)\mathrm{Ad}^T_{(g_{ww_1}^{-1})} K_{s_{12}} \mathrm{Ad}_{(e^{-\hat{\xi}\theta_{eh_{12}}})} & \left(I - \mathrm{Ad}^T_{(g_{h_2o}^{-1}\cdot g_{h_1o})}\right)\mathrm{Ad}^T_{(g_{ww_2}^{-1})} K_{s_{21}} \mathrm{Ad}_{(e^{-\hat{\xi}\theta_{eh_{21}}})} & \mathrm{Ad}_{(e^{-\hat{\xi}\theta_{ee}})} \end{bmatrix} \tag{32}$$

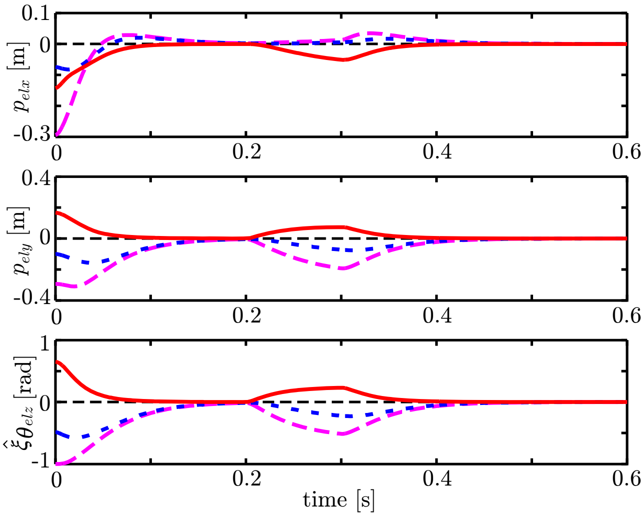

Fig. 7. Control error e_{h_1} (Dashed) and e_{h_2} (Dotted), and the synchronization error $e_{s_{21}}$ (Solid) with the proposed control law adding disturbance

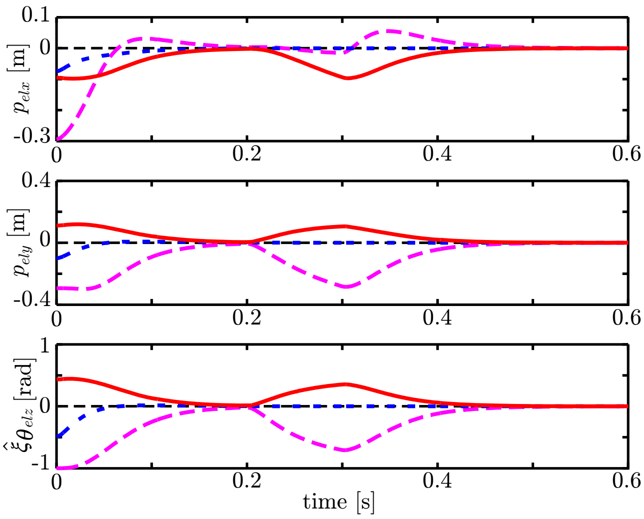

Fig. 8. Control error e_{h_1} (Dashed) and e_{h_2} (Dotted), and the synchronization error $e_{s_{21}}$ (Solid) with the non-synchronized control law adding disturbance

0.2–0.3 [s]. Figs. 7 and 8 illustrate the errors in the case of adding a force disturbance. These results are different from those in Figs. 5 and 6, due to adding the disturbance after 0.2 [s]. Fig. 7 shows that the added force disturbance does not greatly affect the hand control error e_{h1} and the synchronization error e_{s21} under the proposed synchronized control, compared with Fig. 8 in the case of the non-synchronized control. It should be noted that the magnitude of the error e_{h_1} is specially small after adding the disturbance, since the control law is designed by also considering the interaction between manipulators. Our proposed controller reduces the magnitude of the error for the whole system at the small expense of the motion of the manipulators which are not added the force disturbance, as a result, the synchronized visual feedback system becomes robust against the disturbance input. This validates one of the expected advantages of the mutual synchronized control for the visual feedback system.

V. Conclusions

This paper considers synchronized visual feedback control for eye-to-hand systems. In our proposed system, we can treat not only the tracking problem but also the synchronized one, since it consists of the synchronization error system. Based on passivity and dissipative systems theory, stability and L_2-gain performance analysis for the synchronized visual feedback system are discussed. Finally simulation results are shown to verify the stability and the performance of the proposed method.

References

[1] F. Chaumette and S. Hutchinson, "Visual Servo Control, Part I: Basic Approaches," *IEEE Robotics & Automation Magazine*, Vol. 13, No. 4, pp. 82–90, 2006.

[2] F. Chaumette and S. Hutchinson, "Visual Servo Control, Part II: Advanced Approaches," *IEEE Robotics & Automation Magazine*, Vol. 14, No. 1, pp. 109–117, 2007.

[3] G. Flandin, F. Chaumette and E. Marchand, "Eye-in-Hand/Eye-to-Hand Cooperation for Visual Servoing," *Proc. 2000 IEEE International Conference on Robotics and Automation*, pp. 2741–2746, 2000.

[4] V. Lippiello, B. Siciliano and L. Villani, "Position-based Visual Servoing in Industrial Multirobot Cells using a Hybrid Camera Configuration," *IEEE Trans. Robotics*, Vol. 23, No. 1, pp. 73–86, 2007.

[5] T. Murao, H. Kawai and M. Fujita, "Passivity-based Control of Visual Feedback Systems with Dynamic Movable Camera Configuration," *Proc. of the 44th IEEE Conference on Decision and Control and European Control Conference*, pp. 5360–5365, 2005.

[6] T. Murao, H. Kawai and M. Fujita, "Predictive Visual Feedback Control with Eye-in/to-Hand Configuration via Stabilizing Receding Horizon Approach," *Proc. of the 17th IFAC World Congress on Automatic Control*, pp. 5341–5346, 2008.

[7] A. Rodriguez-Angeles and H. Nijmeijer, "Mutual Synchronization of Robots via Estimated State Feedback: A Cooperative Approach," *IEEE Trans. Control Systems Technology*, Vol. 12, No. 4, pp. 542–554, 2004.

[8] E. Kyrkjebø, K. Y. Pettersen, M. Wondergem and H. Nijmeijer, "Output Synchronization Control of Ship Replenishment Operations: Theory and Experiments," *Control Engineering Practice*, Vol. 15, No. 6, pp. 741–755, 2007.

[9] S.-J. Chung and J.-J. E. Slotine, "Cooperative Robot Control and Synchronization of Lagrangian Systems," *Proc. of the 46th IEEE Conference on Decision and Control*, pp. 2504–2509, 2007.

[10] D. Sun and J. K. Mills, "Adaptive Synchronized Control for Coordination of Multirobot Assembly Tasks," *IEEE Trans. Robotics and Automation*, Vol. 18, No. 4, pp. 498–510, 2002.

[11] D. Sun, X. Shao and G. Feng, "A Model-Free Cross-Coupled Control for Position Synchronization of Multi-Axis Motions: Theory and Experiments," *IEEE Trans. Control Systems Technology*, Vol. 15, No. 2, pp. 306–314, 2007.

[12] R. Murray, Z. Li and S. S. Sastry, *A Mathematical Introduction to Robotic Manipulation*, CRC Press, 1994.

[13] M. Fujita, H. Kawai and M. W. Spong, "Passivity-based Dynamic Visual Feedback Control for Three Dimensional Target Tracking: Stability and L_2-gain Performance Analysis," *IEEE Trans. Control Systems Technology*, Vol. 15, No. 1, pp. 40–52, 2007.

[14] H. Kawai, T. Murao and M. Fujita, "Passivity-based Control and Estimation of Dynamic Visual Feedback Systems with a Fixed Camera," *Proc. of the 43rd IEEE Conference on Decision and Control*, pp. 4022–4027, 2004.

[15] F. Bullo and A.D. Lewis, *Geometric Control of Mechanical Systems*, Springer–Verlag, 2004.

[16] A. van der Schaft, *L_2-Gain and Passivity Techniques in Nonlinear Control* (2nd ed.), Springer–Verlag, 2000.